2002

Impact Spherules From Western Australia: A Textural Analysis of Really Old Tiny Rocks

Dawn C.S. Ruth
Oberlin College

Impact Spherules From Western Australia:

A Textural Analysis of Really Old Tiny Rocks

Dawn Sweeney

Honors Thesis

Geology Department

May 2002

Abstract

The fourth shale macroband of the Dales Gorge Member of the Brockman Iron Formation in the Hamersley Basin in Western Australia contains a 2.49 billion years-old impact ejecta layer (Hassler and Simonson, 2001). The S4 layer is the least studied Paleoproterozoic impact layer in the Hamersley Basin. It displays textures and replacement minerals not seen in other layers. Analysis of this layer will help our understanding of the processes that form impact ejecta, especially in the Paleoproterozoic.

It is believed that these ejecta settled in a deep basin environment; laterally extensive beds and mud-sized grains are evidence of the deep basin setting. Samples were chosen based on density of ejecta within the layer. Furthermore, the ejecta exhibited good internal textures. Also, samples were taken from two outcrop sites, Dales Gorge and Yampire Gorge, and one core site, Tom Price.

This impact ejecta layer is made up of two distinct populations that are coarse to very coarse sand sized grains, an angular population and a splash form population. Splash forms are circular, teardrop or oval shaped grains while angular grains usually have boxier shapes. Evidence, in the form of specific crystal morphologies, such as swallow-tail terminations and bowties, is present to support the hypothesis that the target rock was basaltic. Broken splash forms with rims that have devitrification textures are present. Analysis shows that these grains devitrified before breakage occurred. This observation helps to understand the processes that form the splash forms. Mineral compositions vary between the outcrop sample and the core sample. In the former, oxidized stilpnomelane and potassium feldspar are the secondary minerals. However at Tom Price, the secondary mineral is unoxidized stilpnomelane. Different diagenetic environments are obviously at work between the DG/YG sites and the Tom Price. A comparison of the S4 layer with other studied impact ejecta shows that composition, size and internal textures varied from ejecta layer to ejecta layer.

Introduction

Big strides have been made in our knowledge of Phanerozoic impacts, especially the Cretaceous-Tertiary event, but our understanding of Proterozoic impact and impact ejecta is still very limited. For example, the presence of an impact crater greatly aids in understanding the composition of ejecta, which in turn, helps to understand the formation of ejecta; certain compositions will cool differently, giving different textures in the ejecta. The crater also provides information about the effects of such an impact, the K-T event occurred on a carbonate platform. When it was impacted, the carbonate vaporized into greenhouse gases, thus increasing the global temperature. However, due to erosion or an oceanic impact, Proterozoic craters and even ejecta layers are few and far between. We can also study the ejecta found in the rock record as an alternate source of information on Proterozoic. This, of course, also has its limitations, e.g., diagenetic replacement and tectonic deformation. While these problems are sometimes difficult to resolve, important information can still be gleaned from these ejecta.

The Hamersley Basin, famous for its banded iron formations (BIF) (Simonson et al., 1993), should also be famous for its impact ejecta layers. At least two Archean layers and a third Paleoproterozoic layer have been found recently within the Hamersley Basin. These three layers occur within a time span of 140 million years. According to Chapman and Morrison (1994), this represents a recurrence interval which is roughly comparable to K-T magnitude impacts in the Phanerozoic. It is impressive that three layers of this size have been preserved within one basin. The youngest of the three was found in the most famous of the banded iron formations. Within the fourth shale (S4) macroband of the Dales Gorge Member of the Brockman Iron Formation, there lies a spherule-rich bed of coarse to very-coarse sand sized sediments (Hassler and Simonson, 2001). A macrobands, is a term coined by Trendall (1983) and refers to the entire spherule layer and is based on thickness. The mesoband is the basic unit, and ranges in thickness from millimiters to decimeters. Even though new geochemical evidence clearly indicates the S4 layer consists of impact ejecta (MacDonald and Simonson, 2002), it has subtly different textures compared to

other impact spherule layers found in the Hamersley Basin. Moreover, its textures are much different than impact spherules layers found in the Phanerozoic as well (Simonson and Harnik, 2000). The mineralogy of the S4 layer is also different from the other spherule layers, perhaps due to its position in a banded iron formation (Hassler and Simonson, 2001). Basically, it is the least understood of the impact spherule layers within the Hamersley Basin, probably because it has been studied the least. I undertook an extensive petrographic analysis of several samples from the impact spherule layer in the S4 macroband in the Dales Gorge Member of the Brockman Iron Formation in the Hamersley Basin of Western Australia. In this paper I will attempt to classify the different types of ejecta, address composition of the target rocks and diagenetic replacement of the ejecta, and make a comparison with other studied impact spherules layers.

Geological Setting

The Brockman Iron Formation is part of the larger Hamersley Group (Trendall, 1983). The Hamersley Group rests on the Pilbara craton, which is one of the two oldest continental crustal blocks in Australia (Trendall, 1983). The layers within the Hamersley Group exhibit classical basinal successions such as laterally extensive, thinly-laminated, fine-grained bedding interspersed with turbidites (Hassler and Simonson, 2001). While this Group has many iron formations, other types of strata are abundant as well. For example, the Brockman Iron Formation is underlain by argillite with interspersed chert and carbonate of the Mt. McRae Shale (Simonson, 1992). Furthermore, overlying the entire Brockman Iron Formation is another BIF, the Weeli Wolli Iron Formation. Directly above that is the volcaniclastic Woongarra bed (Simonson, 1992). See Simonson et al. (1993) for a nice stratigraphic column of the Brockman Iron formation.

The following description is summarized from Trendall (1983). The Brockman Iron Formation consists of four members: the basal Dales Gorge Member which is overlain by the Whaleback Shale

Member, another BIF the Joffe Member and the Yandicoogina Shale Member. Within the Dales Gorge Member lie meter-scale shale macrobands, the fourth macroband from the base being the location of the impact spherule layer of interest. The Dales Gorge Member is the only BIF in the Hamersley Group to have alternating bands of shale and banded iron formations; there are seventeen BIF macrobands and sixteen shale macrobands.

The S macrobands within the Dales Gorge Member are originally volcanic as is evidenced by volcanic shards (LaBerge, 1966). These beds consist of thinly bedded stilpnomelane-bearing shale with some interbanded chert and siderite (Trendall, 1983). Local occurrences of limestone and breccias were also observed. The BIF macrobands are alternating mesobands of chert and fine-grained iron-rich material such as hematite, siderite and other iron-rich minerals (Trendall, 1983).

It is believed that these strata were deposited in a deep shelf environment because they consist almost entirely of thinly laminated mud layers, coarse grained strata are rare, beds are laterally extensive and wave-forms are absent. However, the spherule layer seems to have been laid down in a different sedimentary regime (Hassler and Simonson, 2001). The spherule layer itself consists of coarse to very coarse sand, made up predominantly of the impact ejecta. The possible wave generated structures and dune-like bedforms found within the layer were not observed anywhere else in the formation (Hassler and Simonson, 1992).

Methods

To determine the relative abundances of different types of ejecta in the S4 layer, I made point counts on fifteen slides from a total of seven samples collected at three locations which had well-preserved textures. At least four hundred points were counted on each of the seven samples (Table 1, Fig.1).

The S4 layer consists of a well-sorted coarse to very coarse grained sand made of impact ejecta and shale fragments. In preliminary counts of slides from Yampire Gorge, it was found that impact ejecta make up 65% of the layer whereas 22% is cement and the other 13% is clasts and crystals such as shale fragments and secondary calcite rhombohedrons.

Two major categories were constructed based on morphology of the impact ejecta. Splash forms is the first category. Any grain exhibiting a circular shape in a two-dimensional cross section was considered a splash form. An oolitic origin was ruled out because the internal textures are neither concentric nor is the radial pattern exhibited radiating outward from the center of the grain. Any grain with a rounded end, such as a teardrop or broken spherule, and oval shapes were considered splash forms (Figs 2 & 3). Angular grains is the other category; any grains with jagged edges, corners, long straight edges that do not turn into an arc, as in a tear drop, were considered for the category. In other words, the angular grains should look similar to typical lithic fragments. However, to differentiate between actual lithic fragments and angular grains and also between different types of splash forms, the two main categories were subdivided into several subcategories based on internal texture of the grain. In the S4 layer, lithic fragments are rip-up clasts of shales that have been reworked. The angular grains show igneous textures similar to those found in volcanic rocks.

To be counted in either the splash form category or the angular category, a grain must fit into one of the determined subcategories based on texture; if it exhibited a shape but not a determined texture, then it was placed into the indeterminate category. These textures were determined by inspection using a transmitted light, petrographic microscope.

Populations for non-circular splash forms and broken, rimmed splash forms were also obtained with point counting. Internal textures were ignored for this count of non-circular splash forms, morphology was emphasized because I wanted to concentrate on the different splash form shapes

exhibited in the layer. First I did the point count based on the criteria above; I only distinguished between angular and splash form grains. I then went back and focused in on the splash forms, using the same grid I used for the first point count, I counted the number of non-circular splash forms and number of broken splash forms. Teardrops, ovals, barbell and elongate splash forms are considered part of the non-circular splash form group. Broken splash forms had to have rims on the original edge of the grain but not on the fracture edge to be counted in the broken splash form category.

During the first count, the cement abundance of the layer was determined. Cement is any mineral that fills void space and can be recognized by radial textures near the grain boundaries. The cement in the S4 layer is stilpnomelane, an iron rich micaceous mineral. In the impact ejecta, the radial textures observed are usually are secondary potassium feldspar based on optical analysis. One sample, 96461, from Yampire Gorge was used to determine the cement volume and was determined to be 22% by volume. The focus of this study is on the ejecta within the layer, therefore this measurement of the cement was assumed for the entire layer.

Grains that exhibited vesicularity were also tallied during the point counts. Vesicles are very small, round or oval shaped areas within a grain that has smooth sides, often exhibiting a radial texture where the stilpnomelane would radiate toward the center from the vesicle boundary.

The dimensions of the impact ejecta were also measured on the microscope. For each clast, I measured the longest dimension called the major axis and the one perpendicular to it called the minor axis. The ten largest splash forms and the ten largest angular grains were both measured from at least one sample at each site. I also estimated the roundness of splash forms and angular grains using a scale from 0.1-1.0 with 0.3 being subrounded. Measurements were taken by visual comparison to a template of silhouettes provided by Bruce Simonson, a subset of which is found Figure 24 in Pettijohn (1949).

To test the similarity of random textures in splash forms versus the angular grains, I measured the lengths of crystals in selected examples of both types of grains. Measurements were only taken on splash forms with at least twenty crystals visible in plane polarized light. Angular grains are usually smaller, so I measured ten crystals as long as they were visible. The lengths of crystals were measured along their longest axes. I measured crystals in splash forms from samples 96460 Yampire Gorge (YG), 96461 YG and 96466 Dales Gorge (DG) and angular grains from 96466 DG.

All length measurements were obtained with the reticle on the eyepiece. Crystal length measurements were taken at x400, x10 eyepiece and x40 objective; the graduate ruler was 250 micrometers long. Impact ejecta size measurements were taken at x40, x4 objective and x10 eyepiece; the graduated ruler was 2.5 mm long. Measurements were rounded to the nearest tic which was, 2.5 microns at the x400 magnification and 25 microns at the x40 magnification.

Results

In the S4 layer, two types of ejecta were found, both in the coarse to very coarse sand size range. Of the entire layer, 65% by volume is interpreted as impact ejecta of some sort. 23% by volume in the one sample counted, 96461 YG, consists of stilpnomelane cement. This cement abundance is the same as the porosity of a well-sorted sand that is slightly compacted. The remainder consists of shale fragments and interstitial cement which is primarily stilpnomelane. Furthermore, diagenetic calcite and opaques are present; the calcite replaces both cement and the margin of non-impact and impact clasts. Calcite grains that replaced splash forms were considered splash forms whereas the calcite that replaced cement was placed into the third category. The final 12%, by volume, of the sample is made up of shale fragments, diagenetic calcite and opaques. Since the calcite probably replaced the cement, the cement abundance may be slightly higher. Pressure solution is evident with some long grain contacts between impact ejecta.

Non-shale grains were interpreted as ejecta particles in part on the basis of their splash form shapes, that range from spherical to elongate, teardrop and dumbbell shapes. Internally, such grains display textures similar to volcanic rocks. Grains with other shapes in the S4 layer have also been interpreted as ejecta. These types of grains have been interpreted as ejecta in other layers as well (Simonson et al., 2000b). Also, observations of angular grains fused with splash form grains supports the hypothesis that these grains formed from the same event, thus ruling out a volcanic origin. With respect to the splash forms, the abundance of spherical shapes is inconsistent with known volcanic layers (Hassler, 1993). The main piece of evidence that indicates these clasts have extraterrestrial origins is their geochemical makeup. MacDonald and Simonson (2002) show that the S4 layer has abundances of platinum group elements that are found only in cosmic bodies. The non-splash form ejecta are collectively referred to as angulars.

Splash Forms

Most of the grains counted in the S4 layer are splash forms with circular cross sections. The roundness values of the splash form grains ranged from 0.5-1.0 with an average of 0.77 and their aspect ratio averaged approximately 0.78. The presence of shapes such as teardrops, dumbbells, ovals and elongate grains is the reason this aspect ratio is not closer to one (Fig. 2). Also observed were grains that seem to have been smashed together. These are believed to have been two splash forms that were agglutinated during flight. Size measurements are of the largest grains in each shape category. The results presented are not meant to be representative of the entire layer, rather a reasonable estimate of the range of ejecta sizes. In a random two-dimensional cross section, the smallest grains could be a slice through the very tip of a grain, thus skewing the measurement toward the smaller sizes. However, measuring the larger sizes set a maximum limit for the ejecta in the layer. The major axis of all the splash forms ranged from 0.34 mm to 2.1 mm, the average length being 1.4mm.

Splash form grains display a variety of internal textures. Listed below are the six categories I broke them into and the defining characteristics of each textural type.

Radial- these grains have fibrous to lath-shaped potassium feldspar crystals radiating inward from their grain boundaries filling the entire cross section (Fig. 3a, 3b). Grains with spherulitic textures, where laths radiate from a central point and not the boundary, were included in this category. A lath is a crystal that is much longer than it is wide. For example, the length of one crystal measured was approximately 50 microns, but its width was 2.5-5.0 microns. The crystal sizes are comparable to those found in the random textured grains. The radial aggregates also showed sweeping extinction.

Random- these grains had potassium feldspar lath-shaped crystals that were either randomly oriented or slightly aligned comparable to a trachytic texture in a volcanic rock (Fig. 4a, 4b). The laths varied in length up to a maximum of approximately 0.15 mm. Also included in this category are grains that were mostly potassium feldspar and exhibited random textures in cross polarized light, but the crystals were not discernable; these grains make up approximately 1.0% of the entire layer. Various crystal morphologies were observed in the random textured grains. Hollow crystals, swallow-tail terminations of plagioclase, rosettes and bowties are all present in the random textured grains; they all were potassium feldspar. These textures are typical of crystals grown from a basaltic melt during quench (Bryan, 1974, Lofgren, 1980, Lofgren, 1977). Quench textures form when a melt is cooled very quickly.

Rimmed- these grains contained a core of stilpnomelane and a rim of potassium feldspar. The exact location of the core varied from grain to grain. In one grain, the core would be in the center while in another grain the core would be slightly off center. Core shapes ranged from circular to more asymmetrical shapes such as u-shapes; texturally the cores would display a void-filling radiating texture similar to cement textures. Sometimes, the stilpnomelane would be sheet like with no stilpnomelane laths visible. In some splash forms, the stilpnomelane would radiate to the center but leave a void space.

The textures of the rims ranged from radial to random but more often than not the rims displayed radial textures with the core/rim interface edges being scalloped. This scalloping is referred to as botryoidal in the literature. Often more than one core was observed in one grain. Thin bands that bisected the cores were present in many rimmed grains. Opaques and potassium feldspar usually formed along the center of these bands, displaying radial textures, perhaps showing there is some sort of boundary present. This banding makes up approximately 5% of the splash form population.

All stilpnomelane- these grains consist entirely of stilpnomelane. Two different types of textures were observed in these grains. First, some grains would look like a flat sheet of stilpnomelane. There are no radiating patterns or laths found in this type of ejecta. In the second type of grain, the stilpnomelane formed a spherulitc pattern with many stilpnomelane laths radiating from a central point; many of these spherulites were located in the ejecta.

Indeterminate- the internal texture of these grains was obscured beyond recognition by fine inclusions of opaques. Potassium feldspar was identified in these grains.

Flow Banding and Spots- Any stilpnomelane pattern that did not fit into the rimmed or all stilpnomelane categories falls into this category. This texture only occurs in the angular grains. These grains exhibit flow banding. Flow banding takes the form of a swirling pattern in the grain, usually outlined by stilpnomelane (Fig. 5); potassium feldspar is also present in the form of crystal laths that usually show random textures. Other textures observed included spots of stilpnomelane within the ejecta boundaries.

Other textural characteristics not incorporated in the categories described above were also noted during the point counts. One such textural feature would be vesicles. About 6% of the splash form population and 18% of the angular population had at least one vesicle present in the grain (Table 2a, 2b). Vesicles formed mostly in the random textured grains. Vesicles were found near the edges of the grain and are filled with stilpnomelane with a void-filling radiating texture similar to the rims above. An

opaque phase was found both on the margins of the grains and inside the ejecta as well. The shapes of the opaque crystals ranged from euhedral crystals found in the random textured splash forms to rod shapes found in the circular centers of the splash forms. Often these opaques would outline the boundaries of discrete crystals in the random textured grains. Opaques were also common along the micro-fractures in the splash form grains. Opaques are not very abundant in the radially textured splash forms. Sometimes, a line of small opaque grains would be found along the long axis of a discrete lath, perhaps indicating that the lath was hollow.

Compositionally, the majority of the splash form grains in the surface samples consisted of potassium feldspar, oxidized stilpnomelane and minor opaque phases. However, not all the samples analyzed came from outcrops. The Tom Price site, the samples, which came from a core, were completely unoxidized stilpnomelane and minor opaques with little to no potassium feldspar. The observed abundance of random textured splash forms is lower in this layer because the green color in the plane polarized light made it difficult to discern random textures.

Finally, broken splash forms make up about 13% of the splash forms in the layer. The shapes of the grains prior to breakage ranged from the teardrop to perfectly circular (Fig. 6). In many of the broken splash forms, the grain would have a stilpnomelane core with a partial rim of potassium feldspar. In every case, the rim would extend along the original curved surface of the grain, whereas no rim whatsoever was observed on the broken edge.

Angular Grains

The largest angular grains were generally smaller than the largest splash forms as reflected in major axis lengths ranging from 0.43mm to 1.8mm with an average of 1.1mm. Their aspect ratio is 0.64 which is slightly more elongate than the splash forms and the roundness is significantly lower, ranging from 0.2-0.6 with an average of 0.34. While the more rounded angular grains have similar roundness

values to the more angular splash form, none of the angular grains displayed the shapes associated with splash forms. That is, the angular grains never have circular, teardrop shaped or oval shapes. Instead, their shapes are more boxy and pointed.

I was able to use the same textural categories for both angular grains and splash form grains because the internal textures of the angular grains are very similar to those of the splash forms. The range of crystal sizes within the random textured angulars is similar to the random textured splash forms. However, there are major differences in the relative abundances of different textural types between the two impact ejecta populations. First, radial textures were quite abundant in the splash forms whereas radially textured angular grains are quite rare and do not show all the textures found in the splash forms, such as the spherulites. Second, in the rimmed grains the rims only partially encircle the angular grains whereas the rims encircle all of the splash form grains. The rims consist of potassium feldspar in both cases, but the rim on the angular grains are generally thinner than those on the splash form grain, making the textures in the rims of the angular grains more difficult to determine.

The cores in both rimmed categories are stilpnomelane and display the same textures throughout the layer. The few radial angular grains showed inwardly radiating fibers. Textures in the all-stilpnomelane category are equivalent in both shape categories as well. Like the splash forms, minor opaques lined the boundaries of impact grains as well as discrete crystals within the grain. Vesicles were also present with the same composition and textures observed in the splash forms; they also only occurred in the random textured grains. Mineralogically, the composition of the splash form and angular grains are similar if not the same.

Replacement

Replacement of original phases by secondary phases is an important issue in the S4 layer. Potassium feldspar is the current silicate phase in these ejecta. However, basaltic magmas usually do not crystallize potassium feldspars. Textures observed indicate the original phase was plagioclase. Likewise, stilpnomelane is not the primary mineral phase but the secondary mineral phase. It replaces the original core in the rimmed grains and the matrix inside the ejecta but not the plagioclase in the ejecta. It is likely that this mineral was a glass.

Since they were both found in outcrop, the Dales Gorge and Yampire Gorge sites had similar diagenetic replacement (Fig. 7a). That is, the plagioclase went to potassium feldspar and the glasses went to stilpnomelane that was then oxidized due to weathering. Furthermore, the potassium feldspar and stilpnomelane are being replaced by calcite. However, Tom Price is located SE of these sites and was found in a core, thus a different diagenetic replacement is observed (Fig. 7b). The plagioclase and the glass in the Tom Price samples has gone to unoxidized stilpnomelane. Calcite replacement of the stilpnomelane is very limited.

Summary of Results

In all of the samples studied, the populations for the different types of splash form remains fairly constant (Fig. 9). Rimmed grains form 60-70% of the splash form population, broken splash forms make up 13.4% of the population and non-circular splash form shapes make up the remaining 26%.

On the grain level, original compositions varied widely as is evidenced by the variety of textures in the ejecta grains. The samples I studied are all similar in composition except for the Tom Price sample. Dales Gorge and Yampire Gorge samples were collected ~25km from each other in the northern part of the Hamersley Basin and have the same composition of potassium feldspar, stilpnomelane and opaques within the grains and abundant calcite in the cement. On the other hand, Tom Price is approximately 100 km SE of these two sites and came from a core instead of an outcrop. This is evidenced by the unoxidized

stilpnomelane, lack of potassium feldspar and lack of calcite rhombs. Different diagenetic conditions may be the cause of the composition discrepancy.

Between the two impact ejecta populations, textural abundances were quite different. In the splash form population, radial textures were more abundant than the random textures by a few percent (Fig. 8a). However, in the angular grain population, the random texture was more abundant than the radial texture, often by an order of magnitude difference (Fig. 8b). Another difference is the abundance of all stilpnomelane grains, the angular population has more than the splash form population. The abundances of the splash form ejecta is fairly constant at all three sites. However, the angular abundances vary more with location. For example, the random textured angulars are more abundant in Yampire Gorge than at Tom Price. Figure 9 shows the geographical distribution of the different types of ejecta for the S4 layer.

Crystal Measurements and Textures

The average length of potassium feldspar laths in the random textured splash forms and angular grains is 0.055mm and 0.050mm, respectively. These measurements were taken from forty-one splash forms and ten angular grains from two sites, Yampire Gorge and Dales Gorge.

Interpretation and Discussion

Composition

Observed textures of the S4 layer indicate the impact ejecta were probably basaltic in composition. When a bolide collides with the earth it vaporizes and rarely leaves fragments. Since the impactor is vaporized, we can infer that the composition of the impact ejecta have a composition similar to the composition of the target rock. In the layer, elongate feldspar crystals are quite common inside an impact grain; many workers site this feature in their studies of basaltic crystallization (Lofgren, 1980; Bryan, 1972; Pearce, 1971; Gélinas and Brooks, 1971; Lofgren and Donaldson, 1977). Swallow-tail terminations are a common texture in many types of basalts (Bryan, 1972; Gélinas and Brooks, 1971; Pearce, 1974).

These types of textures indicate rapid cooling, even quenching, of the liquid (Pearce, 1974). While the crystals may have cooled rapidly, Gibb argues that supercooling in basaltic melts inhibits plagioclase growth and thus growth of plagioclase is more difficult in lower viscosity liquids (1974). With respect to textural variations, perhaps cooling rate is only one of a number of factors. Lofgren (1977) states nucleation history, precooling melting and crystallization are more important than a determined cooling history in terms of textural variation. Gélinas and Brooks confirm this argument with the observation that flow oriented plagioclase crystals tend to occur in rapidly cooled liquids rather than supercooled melts (1971). Rapidly cooled liquids are characterized by skeletal crystals while supercooled liquids are purely glass. It is likely there is a gradient between the rapidly cooled liquids and supercooled liquids. In the S4 layer, there were a few spherules with aligned plagioclase laths (Fig. 3). In this spherule, the laths are aligned along the edge of the central core of the spherule. With that said, it is more likely that these textures were formed by rapid cooling and not supercooling because various crystal morphologies have been observed in the impact ejecta of the S4 layer.

Impact melts provide ample opportunities for crystals to grow. Inclusions of unmelted rock and microscopic particles make for great nucleation sites. Lofgren (1983) states that for supercooled liquids, as impact melts are often seen, plagioclase will only nucleate in heterogeneous liquids; the size of the plagioclase crystals are directly linked to the number of nucleation sites as well. Basaltic liquids are low viscosity magmas. According to Lofgren (1980) nucleation potential increases with decreasing viscosity. The presence of many plagioclase crystals in one spherule indicates many nucleation sites that may lead to more crystals and thus a lower viscosity melt. Further evidence of the impact grains being basaltic is given by visual comparison with other Archean basalts (see Fig. 5, Pearce, 1974).

One concern with this argument is the lack of pyroxene or olivine. If these impact melts were really basalts, then these two minerals should be present. However, olivine and pyroxene have not been

positively identified in some basalts, perhaps due to their lowered liquidus from the quenching process (Pearce, 1974). Pyroxene is also not a prominent mineral in liquidus phase melts according to Bryan (1972). In fact, it is believed that plagioclase was the normal liquidus phase during the Precambrian (Pearce and Donaldson, 1974). Also, as the cooling rate increases, the nucleation temperature decreases thus lowering the liquidus (Lofgren, 1980). Another consideration worth discussing is that many rock types other than basalts may have been melted when the bolide impacted. This would make the composition of the impact melt more of a hybrid between different end members. Despite these hybrids, plagioclase and other silicate minerals are likely to form from the melts because of the relative abundances of silca and the alkali metals in the lithosphere. Also, these melts are quite hot and must cool past the liquidus point of the silicate minerals. Passing the liquidus for the silicates will cause them to crystallize thus reducing the melt's relative concentrations of elements such as oxygen, silicon and the alkali metals. Moreover, this will reduce the likelihood other phases crystallizing.

Botryoidal interfaces between the rims and cores has been observed in the majority of the splash forms. Botryoidal interfaces have been shown to indicate that the core was once glass (Maritinez Ruiz et al., 1997).

Radial textures were more common in the S4 layer than the random textures. In the literature, this texture is referred to as spherulitic and is considered to be a quench texture; increasing supercooling creates the spherulitic texture (Lofgren, 1980). However, Lofgren also claims that spherulites are devitrification textures and attributes them to a slower cooling rate with more water present in the system (1971b, 1971c). Impact ejecta typically have very low water content (Glass et al., 1997), thus water content should not be an issue. However, water content of surrounding rocks and solution will be addressed later.

Formation

While the lunar impact spherules are not comparable in many respects, their formation seems to have some similar characteristics as the S4 impact ejecta. One similarity between the two types of impact grains is the shapes of the majority of the grains and microtektites. For the most part, the S4 grains have good spheroidal shapes. Lunar spherules studied are said to have solidified before landing, thus retaining their spheroidal shape (Symes et al., 1998). It is reasonable to state that the terrestrial spherules found in the S4 layer also solidified before reimpacting with the earth. Within this layer are also broken rimmed spherules. It is possible that thermal stresses, which may occur when hot particles fall into cool water, caused these splash forms to break (Glass et al., 1997). These grains also solidified before reimpacting with earth. The rims, however, do not go all the way around a grain. This indicates that the rimming, and potentially the breakage, occurred before reimpaction; there is no internal deformation of the rims. This rimming also occurs in lunar samples; these samples were also metasomatized before brecciation (Ruzicka et al., 2000). However, metasomatization requires an aqueous solution to cause replacement. Water is not present on the lunar surface, so devitrification must occur because of some other process. Lofgren (1971a) suggests thermal devitrification would cause the change in phase. That is, the melt solidifies and is then reheated when another impact occurs causing the rock to melt and rearrange its crystal structure.

One important observation of impact processes is that the rims on the broken splash forms have radial textures that only occur on the original edge of the grain (see Fig. 6). This is evidence of the rims having already been crystallized before they were broken. Potentially, this may show that crystallization was nearly complete before the ejecta fell to the ground. Crystallization is affected by availability of nucleation sites, cooling rate, and other magmatic processes. The most common texture seen in the rims was radial, which is interpreted as a devitrification texture due to its spherulitic nature. Lofgren (1971b, 1971c) links devitrification to water content in the magma. While impact melts are dry (Glass et al.,

1997), outside sources of water such as precipitation could get into the grain through a fracture and could devitrify a grain if its flight time was long enough. These grains also show two different compositions within the grain. If the grain was mostly crystallized before breakage, then the center must be of different composition to accommodate the different replacement mineral and lack of textures similar to the rims.

Within the community of researchers on impacts, the idea of vapor condensate formation of the impact grains is gaining interest. Smit et al. (1992) predicted that the non-circular splash forms, i.e. teardrops, barbells, etc., were formed from a melt. This is a reasonable assumption because it would be difficult to get those shapes from a vapor. In the same article, he says that the microkrystites, the random textured grains, form in the more energetic part of the plume, the vapor. The idea is that most of the impact plume is vapor (Pope, 2002). As it cools it condenses into little droplets of melt. There are some pieces of evidence that point in the opposite direction for the S4 layer. Of the splash form population ~27% have non-spherical shapes, teardrop, elongate, oval, etc. In the K-T layer these type of splash forms also occur, but are believed to have formed in a melt, not a vapor plume, and are found at proximal distances from the crater (Martinez Ruiz et al, 1997, Smit, 1999). Furthermore, quench textures have been observed within some of the S4 splash forms, whereas in the K-T layer, only distal ejecta contain crystalline textures. Size may be an issue as well. Smaller spherules may form from vapor plumes as in the case of lunar spherules (Ruzicka et al., 2000; Symes et al., 1998, Pope, 2002). However, the size of the S4 impact grains are on the order of millimeters while the lunar spherules are on the order of micrometers and the K-T grains range from 250 microns at distal sites and around a millimeter at proximal sites (Smit, 1999). This indicates melt formation was the primary formation mechanism for these impact ejecta.

Melosh and Vickery (1991) estimated the approximate diameter of the bolide for the K-T strewn field layers by using spherule diameters and predicted the velocity of the bolide to be 20km/s. Their

predictions are remarkably close to the accepted size of the bolide ~10km. Using their equation, I predict the bolide for the S4 impact ejecta had a diameter of ~26.8km. However, in their calculations, they used the smallest size fraction found at distal sites from the crater. I used the average size of the splash form grains in the entire ejecta layer. This could skew the calculation of the size of the bolide toward predicting a larger object. Yet, this diameter of the bolide may be reasonable as is evidenced by the density of the splash forms in the layer and Iridium content. Iridium found rarely on earth surfaces, thus the concentrations of this element are vary small. However, cosmic abundances of Iridium and Platinum Group Elements are much greater than those found on Earth. When a cosmic body such as an asteroid collides with Earth, it brings those cosmic abundances of Iridium. The larger the cosmic body, the more Iridium present; a large spike in Iridium in geochemical analyses is proof of a large body collision with the Earth.

Fracturing and Replacement

In many of the splash forms, fractures are evidenced by differential replacement and diagenetic crystallization of opaques along fracture lines (see Fig. 7a, the teardrop in the center). One example of differential replacement is when the stilpnomelane replaces everything around a crystal except for that crystal (see Fig. 4a, the crystals that border the stilpnomelane core). I believe the reason for this type of replacement relates to compositional differences within the grain. Many studies have been performed on tektites from other impacts to test solution rates (Glass, 1984; Glass, 1986; Glass et al., 1997; Barkatt et al., 1986). In all of these studies it was shown that silica content is a determining factor in the durability of glass. Furthermore, the lower the silica content, the higher the dissolution rate and thus the more replacement. Glass (1984) observed that all dissolution takes place before burial and stops after burial; age is also not a determining variable in solution rates. If a spherule fell onto land instead of the ocean, the solution rates would also be higher; if it fell into the shallow water, the solution rate would be faster

than those that fell into the deep water (Glass, 1986). One factor to consider is the composition of the water Glass used as opposed to Paleoproterozoic water composition. The seawater used in the experiments is modern seawater which is undersaturated in silica due to the presence of diatoms and radiolarians thus making the dissolution of silica faster to accommodate those organisms needs. However, similar dissolution rates occur on terrestrial sites where silica saturation is not as important. Perhaps an analogy can be made between terrestrial dissolution rates and Paleoproterozoic dissolution rates because silica saturation may be more similar.

In the S4 layer, two sites are composed of oxidized stilpnomelane and potassium feldspar while the third is primarily unoxidized stilpnomelane; no potassium feldspar is evident in the Tom Price samples. It is likely that the varying diagenetic environments, i.e., outcrop versus core, are responsible for this difference in composition. In the core, the ejecta were not exposed to rain and the atmosphere. Similarly, the outcrop samples were not subject to the same concentrations of groundwater which has an ion composition different from the atmospheric water.

Comparison with Other Impact Ejecta

Similarities (Table 3)

Cretaceous-Tertiary layer- Microkrystites are abundant in the K-T layer at distances greater than 4000km (Smit, 1999). Furthermore, these impact ejecta contain relict crystalline textures of elongate clinopyroxene crystals and the radial textured grains. The average size is 250 micrometers. At proximal sites, the layer's character changes and includes glassy particles that are larger which include flow banded grains, splash forms and highly vesiculated grains (Smit et al., 1992). 4000km from the crater, ejecta sizes range from 0.9mm to 1.1mm.

The following impact spherule layers are all found in the Hamersley Basin of Western Australia. All of these layers have been dated to Archean. Hassler and Simonson (2001) provide a map of all the following impact spherule layers in the Hamersley Basin.

Carawine Layer- It has been dated to 2.55 Bya (Hassler and Simonson, 2001). With respect to the splash forms, the size range is very similar to that in the S4 layer, 0.25mm-2.5mm, in cross section. Splash forms are present but only constitute 13% of the former melt particles. Textures are simillar as well; the radial texture is found in both the S4 and the Carawine. The composition of the layer is similar as well with potassium feldspar as a primary component. Arc fragments were found in this layer in relatively large numbers. These fragments are pieces of shattered spherules, their presence indicates these broken spherules were once hollow (Simonson et al., 2000).

Jeerinah Layer- It has been dated to 2.63 Bya (Hassler and Simonson, 2001). This layer is on the whole, smaller than the S4 layer. The composition is actually closer to that of the Carawine layer than the S4 layer.

Wittenoom Layer- Its has been dated to 2.54 Bya (Hassler and Simonson, 2001). Like the two previous layers, the textures are very similar. Size of the grains is also very close to that of the S4 layer.

Differences

The primary difference between all of the other layers and the S4 layer is composition. In the K-T layer, the presence of clinopyroxene is a huge difference. First, the K-T layer at first consisted of clinopyroxene and then was replaced to potassium feldspar. In the S4 layer, I believe the initial composition was plagioclase, not pyroxene. This was replaced by potassium feldspar. The usual quench pyroxene morphology is dendritic and feathery (Pearce and Donaldson, 1974). I did not observe any crystal morphologies that were dendritic or feathery. Also, it seems more difficult for clinopyroxene to form in quenched liquids (Pearce, 1974).

Within the other Precambrian layers, none of them have stilpnomelane in the same quantities as the S4 layer. This could be related to location; the S4 layer is located within a banded iron formation and the sheet silicate that formed is iron rich. The other layers with sheet silicates just have muscovite (Simonson et al., 2000b). Another noticable differences is that all the Precambrian spherules have clear spots while the S4 layer does not. These clear spots are vesicles and gas bubbles diagenetically filled with quartz, feldspar, carbonate and muscovite (Simonson et al., 2000). Their presence in these spherule layers but not the S4 layer could mean two things. First the S4 spherules did not have gas bubbles and vesicles. This is not likely because there is evidence of vesicles in spherule and angular grains in the S4 layer. Second, the clear spots of the Carawine, Jeerinah and Wittenoom layers have not been replaced in the same fashion as the S4 layer. This is the more plausible explanation because of the unique stratigraphic position in a banded iron formation.

Texturally, the Carawine layer and S4 are different in various ways. First, random textured grains are more prevalent in the S4 layer. Furthermore, angular grains and splash form grains often have textural similarities in the S4. On the other hand, in the Carawine layer, random textured grains are very limited. Moreover, the angular grains that are present rarely exhibit similar textures to the textures found in the splash forms. In the Carawine, arc fragments were found while they are not present in the S4 layer. Instead, the S4 layer has broken splash forms.

Smit (1999) claims that splash forms cannot form past 4000km. He also observed that microkrystites were not found in the proximal zone. However, in the S4 layer there are both splash forms and microkrystites present. This seems to go against the K-T model that the non-circular splash forms and the microkrystites formed from different processes that put them in different strewn fields. Glass et al. (1997) showed that fragmentation of microtektites is related to distance from the crater; for percentages of broken splash forms comparable to the S4 layer, around 13%, the distance measured

ranged from 2545km to 3982km. The fragments were collected using sieve techniques, whereas I used thin section techniques to determine size. This could pose some problems of comparability with the S4 layer. Smit would place the layer in a proximal location, I place it in a more distal location based on microkrystite population and broken fragment percentages.

Splash Forms vs. Angulars with internally random textures

Analysis of the measurements for the crystal lengths versus clast size for splash form and angular grains brought up some interesting plots for one sample, 96466 (Fig. 10). Within the angular grains, the lengths of the feldspar stay about the same size despite clast size. In contrast to the angular grains, the lengths of the feldspar laths in the splash forms span a broader range of sizes from 41 microns to 78 microns. First, if the angular grains were related to the splash forms, wouldn't their populations be somewhat similar? Recall that in the splash form category internally random textures were ~7% while in the angular category internally random textures were 20%! Second, if the grains were related wouldn't the crystals in the angular grains be more random with respect to grain size? On the other hand, wouldn't the splash form crystals be more regular? Observations of angular grains with agglutinated splash forms indicate that the two types of grains formed in the same event. There are many explanations for this discrepancy in the two populations. One possible explanation is that the angular grains and splash forms are not related; the angular grains could be the target rock that was blown out of the crater but not vaporized or melted. However, this seems unlikely because the angular grains have exhibited crystal morphologies that have been linked with quench textures and seen in the splash forms. Yet the target rock may have had the quench textures when the impact occurred. Glass et al. (1997) provides evidence that unmelted impact ejecta is found only at proximal distances. The S4 layer is interpreted to be at a more intermediate to distal distance from the crater. Another possible explanation is that the angular

grains could be derived from a restricted range of splash forms. Further study is necessary to determine if this hypothesis is true.

The Only Global Model

According to Smit et al. (1992) there are two parts to the K-T ejecta plume, the vapor and the melt. Based on observations of K-T ejecta, it is thought that the two parts of the plume produce different types of ejecta (Smit, 1999, Smit et al., 1992). The less energetic melt produces the glass tektites and tear-drop shaped splash forms while the more energetic vapor produced the microkrystites, the random textured, splash forms (Smit et al., 1992). Since the energies of the two parts of the ejecta plume are much different it is reasonable that the two types of ejecta should not be found in proximity to each other. However, in the S4 layer, both types of splash forms are found next to each other, thus the S4 layer does not fit into the K-T model.

Conclusions

This paper characterized the different types of impact ejecta found in the S4 macroband of the Dales Gorge Member of the Brockman Iron Formation in the Hamersley Basin in Western Australia. Observations show that there are two distinct populations of ejecta, the splash form population and angular grain population which were millimeters in size. Within these populations a variety of textures were classified and analyzed.

1) The random textured splash form and angular grains display crystal morphologies indicative of basaltic melts, thus the ejecta is basaltic. This is supported by a literature review and comparison with Archean basalts and lunar impact ejecta (Pearce, 1974, Pearce and Donaldson, 1974, Lofgren, 1977). The textures formed rapidly but not during supercooling.

2) Broken rims within the splash form population provides evidence that the ejecta were solidified before breakage due to the partial rims having radial textures. This observation provides new information

about the processes that form the splash forms. This new information includes crystallization times of the spherules, i.e. the crystals formed in flight rather than during deposition.

3) Replacement phase is determined by original composition. Plagioclase is replaced by potassium feldspar while glasses are replaced by stilpnomelane. However, site location factors into replacement phase as well. Tom Price samples are replaced by unoxidized stilpnomelane while Dales Gorge and Yampire Gorge are replaced by oxidized stilpnomelane, potassium feldspar and calcite. While this is only a weathering phenomenon, the presence of oxidized stilpnomelane Dales Gorge and Yampire Gorge samples has made observations easier than the unoxidized stilpnomelane in the Tom Price samples.

4) Compared with other studied ejecta layers, the S4 layer has a larger abundance of random textured splash form grains, more stilpnomelane and the presence of angular grains with similar textures to the splash form grains. Splash form grain sizes are comparable for the Hamersley Basin layers and the intermediate distance K-T samples.

5) The S4 layer does not fit into the only global ejecta layer model, the K-T model, based on the observation of tear drop splash forms next to microkrystites in the S4 layer.

Further Work

This study of the S4 ejecta layer is by no means complete. Scanning electron microscope or electron microprobe work would be useful to determine the opaque compositions and exact mineral phases of the layer. This would provide geochemical evidence of the melt composition. Also, knowing the opaque mineral composition would help to determine if the opaques were primary minerals or secondary minerals. Another study of this nature that included more study sites and samples would provide an even broader base for comparison with large ejecta layers like the K-T. A better model for global layers should be developed based on new observations. Finally, continued study of this and other

layers will contribute to our understanding of the processes that occur when a bolide collides with the earth.

Acknowledgements

I would like to acknowledge Ms. Retha Ball for all her help and support during the year, especially with the photocopying and printing. Thanks to Mr. Pete Munk for help with the thin sections. Finally, thanks to Mr. Bruce Simonson for teaching me what it is like to do research and introducing me to the wonderful world of spherules.

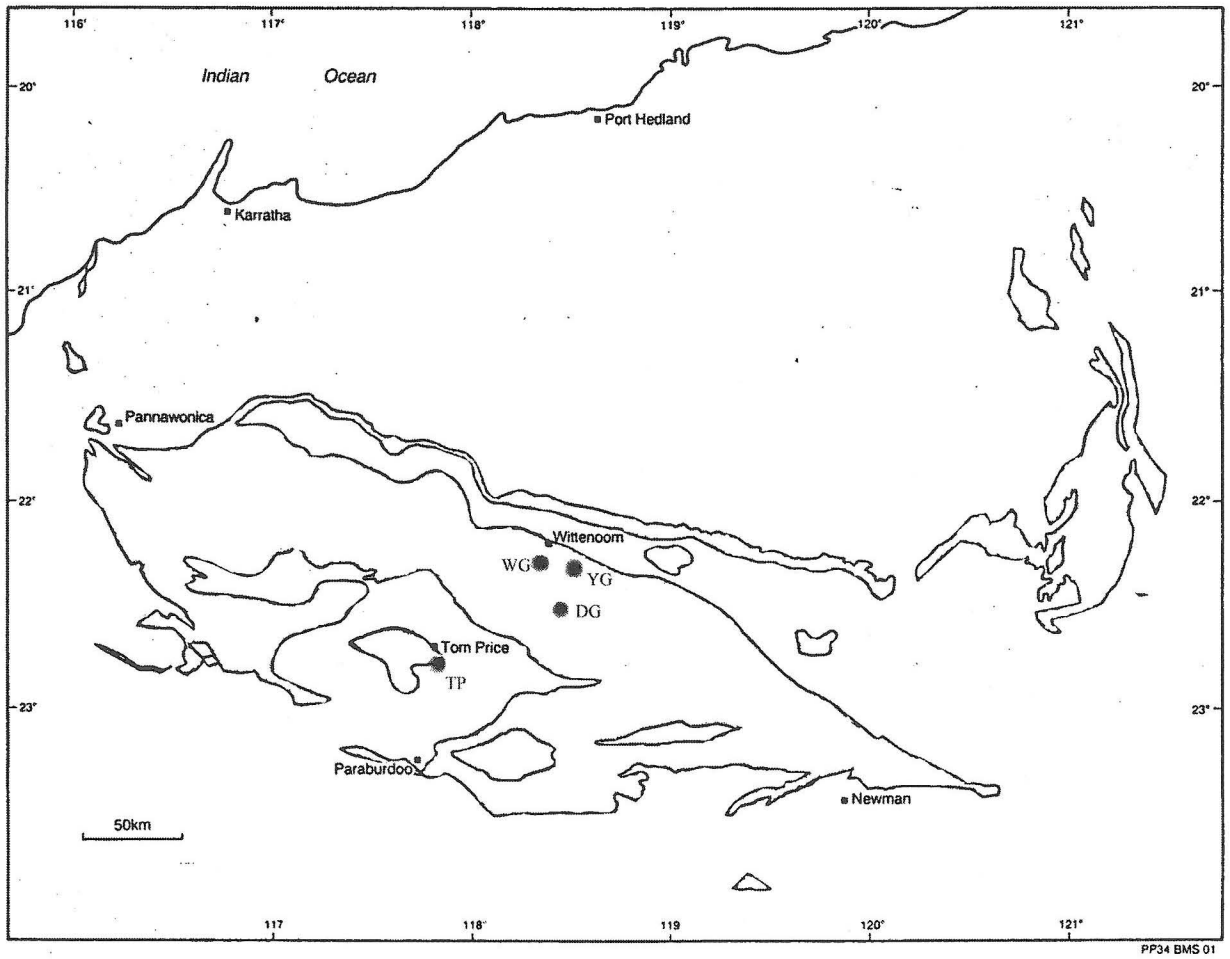

Figure 1- Geological sketch map of the Hamersley Group showing the approximate locations of all study sites (Simonson et al., 1993).

Fig. 2- This is an example of a non-circular splash form; this would be called a barbell/teardrop shape. The core is stilpnomelane and the rims are postassium feldspar. The little black crystals are opaques. Calcite is replacing the stilpnomelane cement and par of the splash form.
Site: Dales Gorge
Field of view: 1.6mm

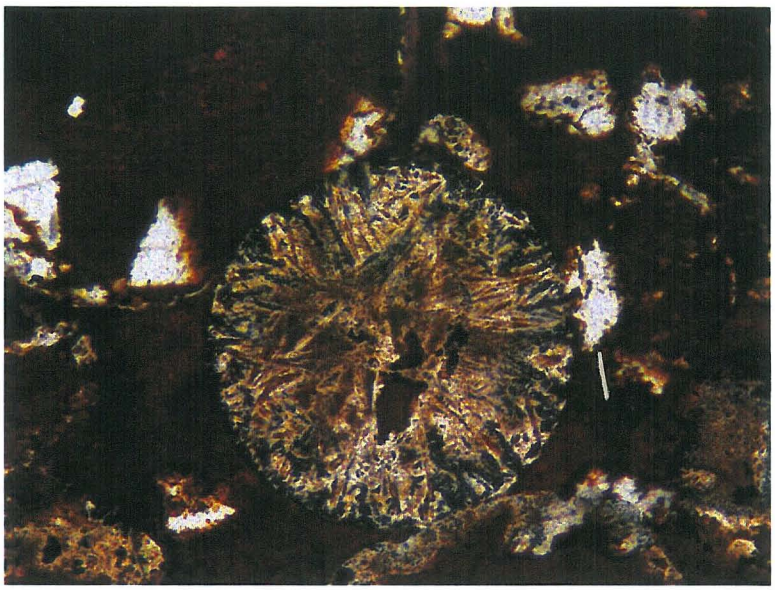

Fig. 3a- This is a typical radial texture in a splash form. The dark crystals are opaques while the euhedral rhombs are secondary calcite. This spherules has a long contact with another grain which is evidence for some compaction within the layer.
Site: Dales Gorge
Field of View: 1.6mm

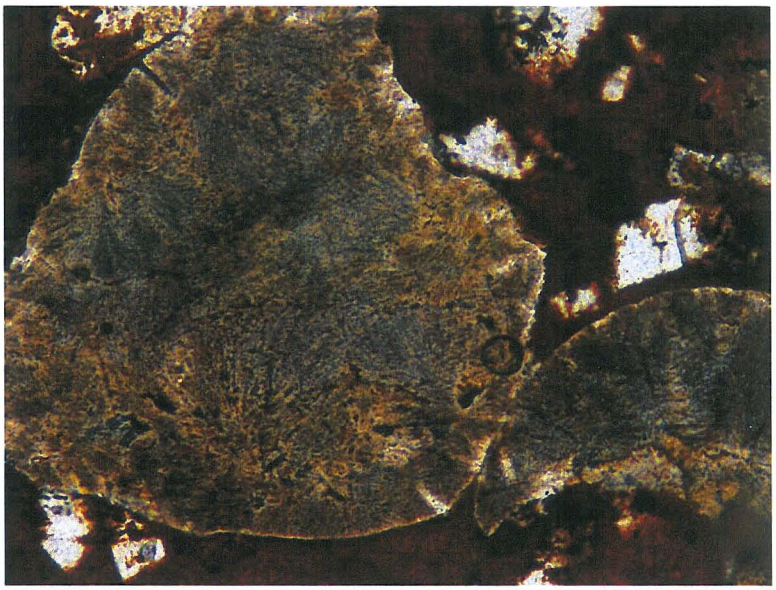

Fig. 3b- This is one of the rare radially textured angular grains. This texture is similar to the one found in 3a but it is a little more feathery.
Site: Dales Gorge
Field of View: 1.6mm

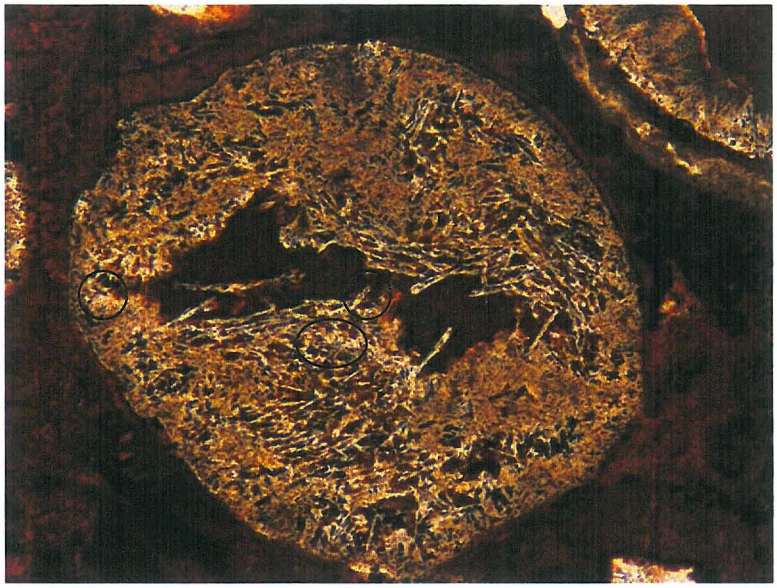

Fig. 4a- This splash form displays random to trachytic textures. The central spots are stilpnomelane while the white areas are potassium feldspar. Note the discrete crystals outlined in the stilpnomelane, this is the oval. Also within this splash form are swallow tail terminations, a crystal morphology linked with quench textures, these are circles.
Site: Dales Gorge
Field of view: 1.6mm

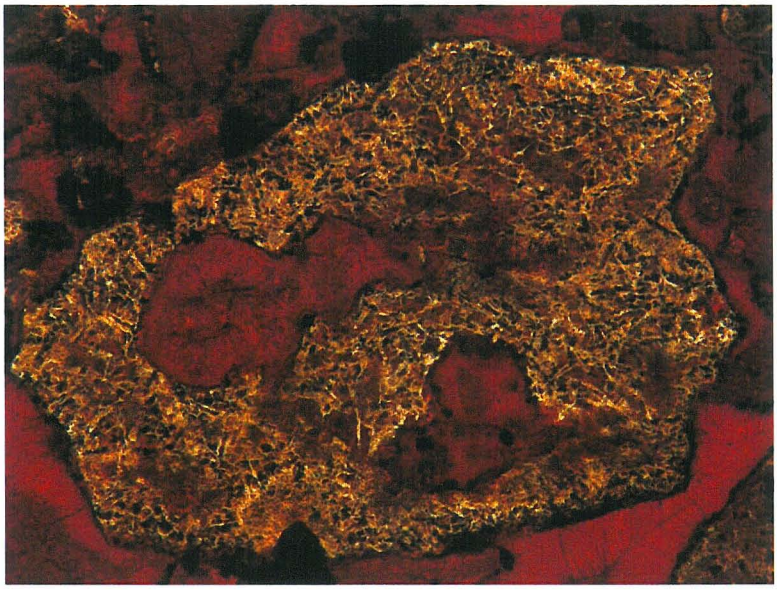

Fig. 4b- This is the same texture yet in the angular ejecta. One thing to note is the texture in this picture is not trachytic but random. Discrete crystals are also outlined in the stilpnomelane here.
Site: Yampire Gorge
Field of View: 1.6mm

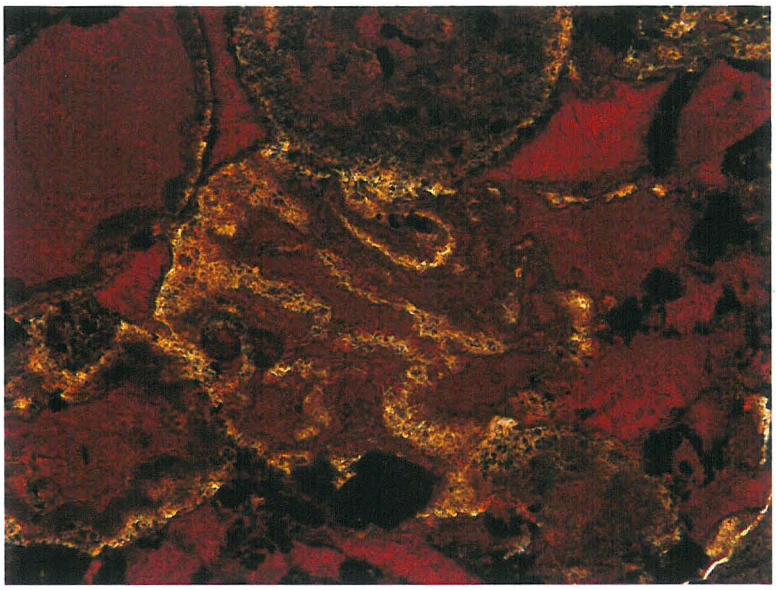

Fig. 5- Flow banding is evident in this grain because of the wavy patterns displayed by the stilpnomelane. This grain is touching several of its nearest neighbors, showing slight compaction of the ejecta layer.
Site: Yampire Gorge
Field of View: 1.6mm

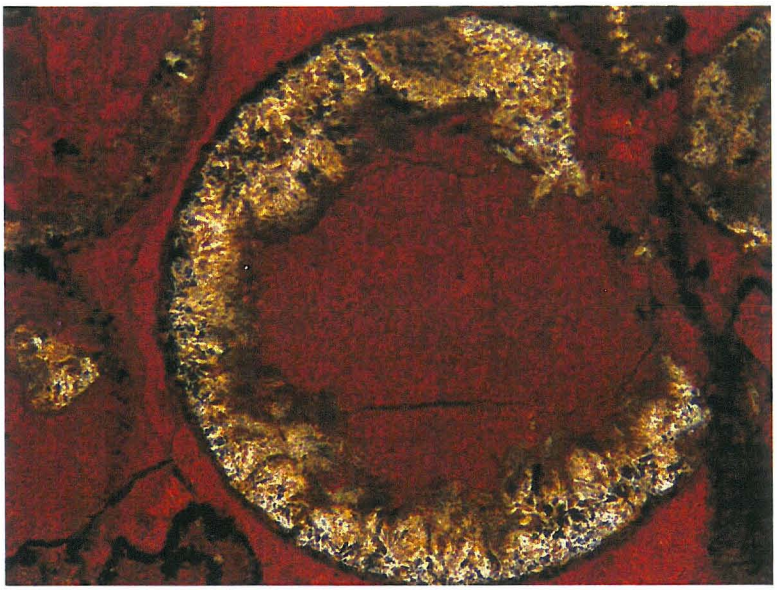

Fig. 6- This grain was broken after its rim crystallized. Evidence is given by the lack of a potassium feldspar rim on the broken edge. This clast displays good radial texture. The core rim interface is considered botryoidal because of its scalloped nature.
Site: Yampire Gorge
Field of View: 1.6mm

Fig 7a- This sample came from the outcrop and is obviously oxidized stilpnomelane. Notice the fractures are also present in the teardrop shaped grain in the center.
Site: Dales Gorge
Field of View: 4.75mm

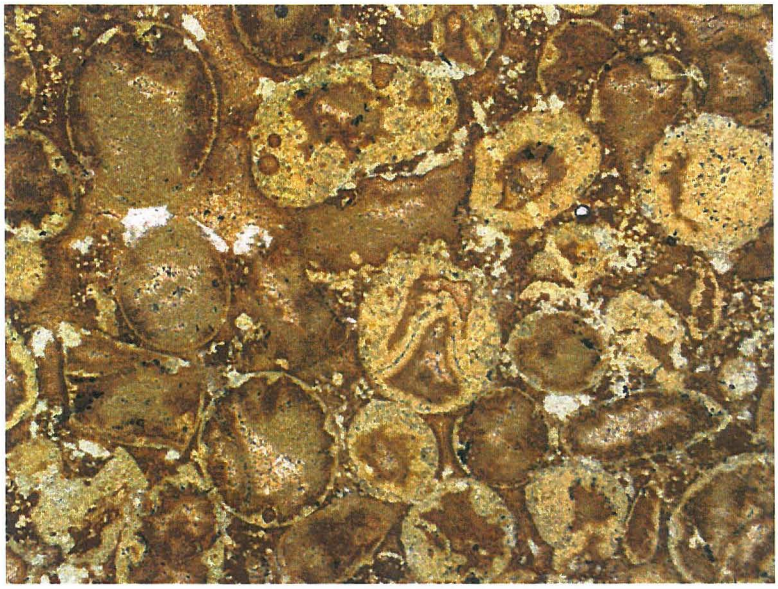

Fig 7b- This sample is from the core which is evident in the green color of the rock, perhaps due to a lack of weathering. The green minerals is unoxidized stilpnomelane. The pale green minerals is also believed to be stilpnomelane. Notice the fracture in the spherule in the center.
Site: Tom Price
Field of View: 4.75mm

Fig. 8a, b - This is a pie chart that shows the relative abundances of the splash forms and angular grains in the entire S4 layer. Category 1) radial textures. Category 2) random texture. Category 3) rimmed grains and Category 4) a combination of the all stilpnomelane and indeterminate categories. In the angular pie chart, category 5 is the flow banded angular grain abundance.

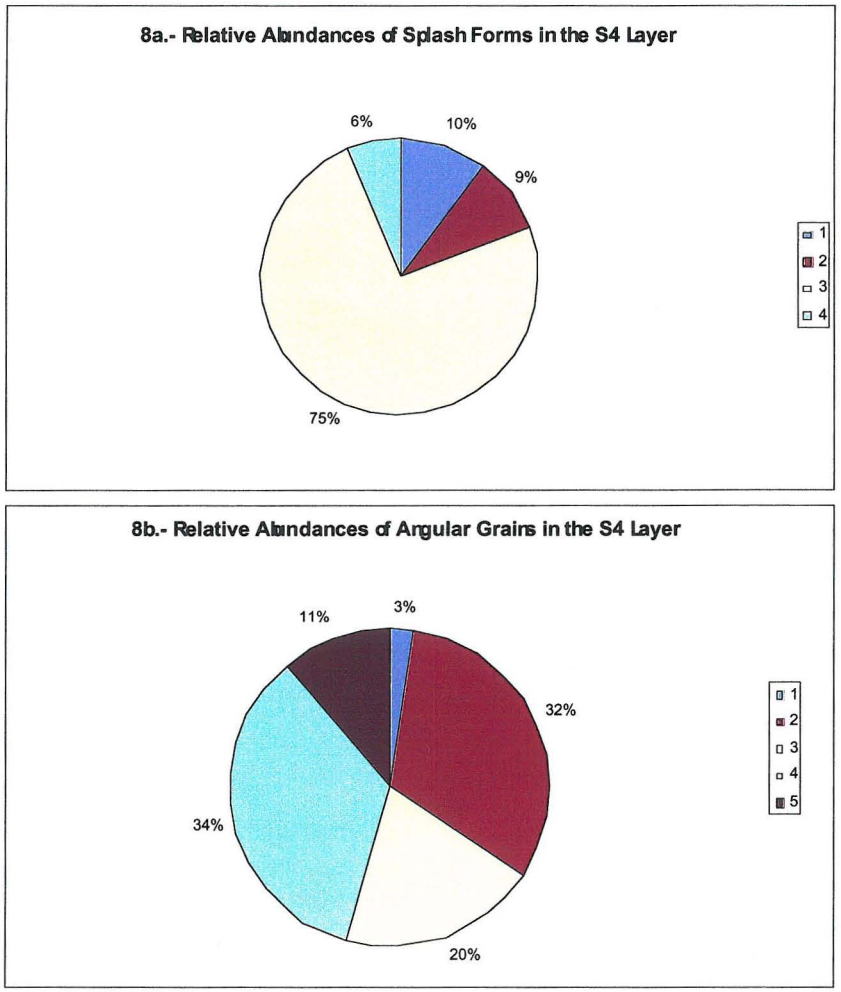

Fig. 9 - Abundances of the ejecta categories throughout the layer. Analysis of these data show that the splash form abundances are fairly constant despite geography. The angular grain abundances vary more with geography.

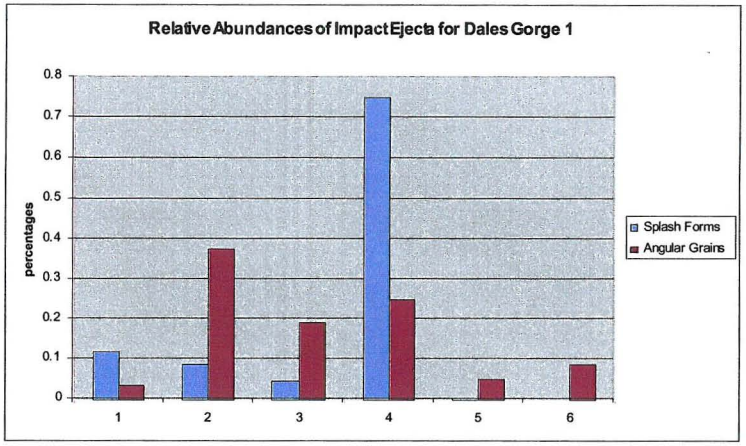

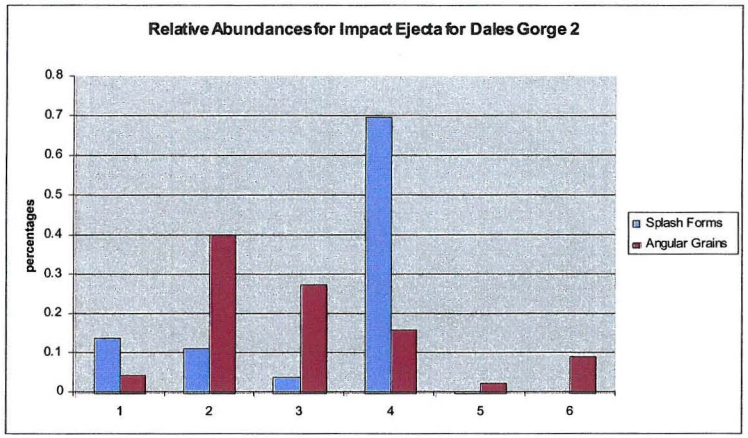

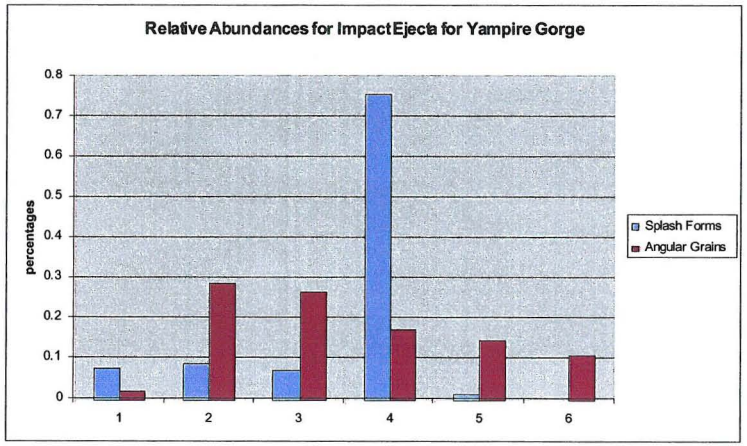

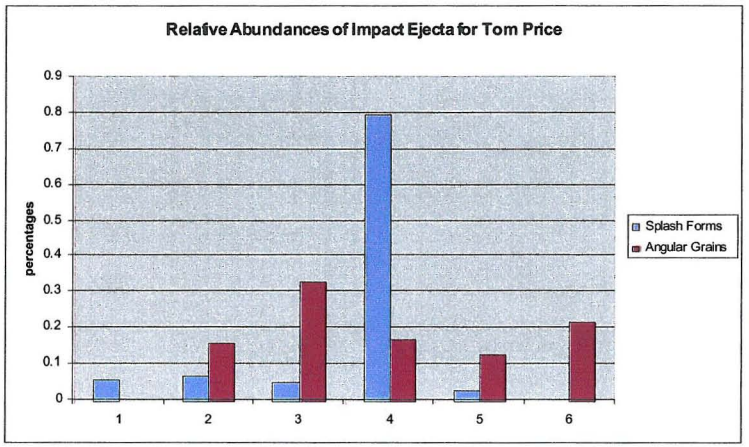

Fig. 10- This graph shows a trend in crystal lengths for one sample, 96466, of the ejecta layer. For crystals in the angular grains, the lengths seem to stay the same despite clast size. On the other hand, the crystals lengths for inside the splash forms is much more random.

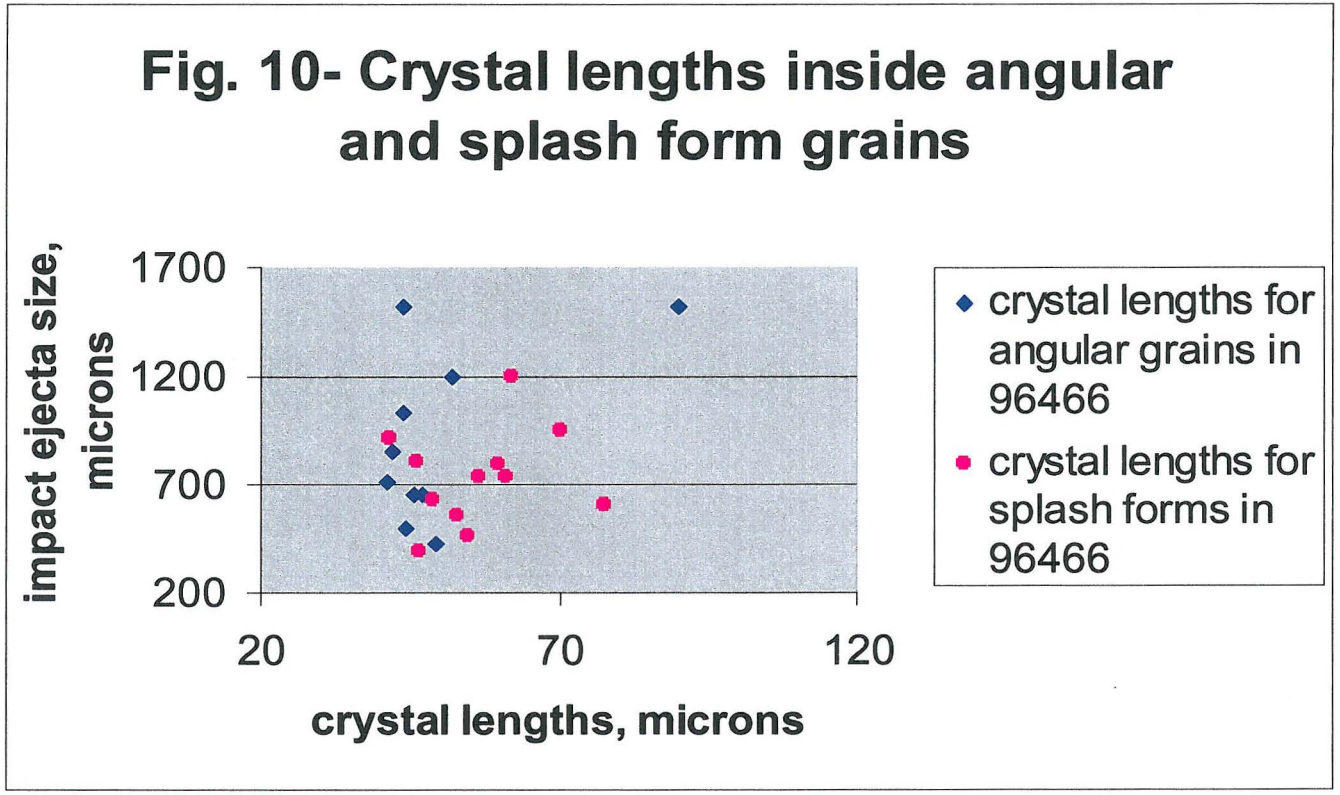

Table 1. This table provides information about the samples used in the point counting.

Site	Information about data collection
Dales Gorge 1	Samples: 96466, 96467, 96468 Two slides for each sample. These samples are essentially from the same location within the site. This site was in outcrop
Dales Gorge 2	Sample: X12-2 Three slides from this sample. This location is approximately 200 meters down gorge from the Dales Gorge 1 location. This site was in outcrop
Yampire Gorge	Samples: 96461, 96460 Two slides for each sample. These samples are essentially from the same location within the site. This site was in outcrop.
Tom Price	Samples: AP-3A, AP-3C One slide per sample. These samples are from the core and therefore the same location within the site.

Table 2a

Abundances of vesicles, broken splash forms and non circular splash forms in the splash form population

	Yampire Gorge, %	Dales Gorge 1, %	Dales Gorge 2, %	Tom Price, %
Vesicularity	13.3	13.9	9.9	16.6
Broken Splash Forms	7.0	5.1	5.5	5.6
Non-Circular Splash Forms	23.4	22.8	27.0	31.1
Average Size	major axis: 1.4mm minor axis: 1.0mm	major axis: 1.3mm minor axis: 1.1mm	major axis: 1.5mm minor axis: 1.2mm	major axis: 1.3mm minor axis: 1.0mm
Ave. Roundness	0.75	0.75	0.78	0.79
Aspect Ratio	0.71	0.85	0.8	0.77
Cement, in preliminary counts	22.5%	n/a	n/a	n/a
Other Fragments, in preliminary counts	12.9%	n/a	n/a	n/a

Table 2b

Abundances of vesicles and size in angular grains

Vesicularity	16.7	18.6	14.9	28.4
Average Size	major axis: 1.0mm minor axis: 0.6mm	major axis: 1.3mm minor axis: 0.9mm	major axis: 1.1mm minor axis: 0.7mm	major axis: 1.2mm minor axis: 0.7mm
Ave. Roundness	0.37	0.34	0.31	0.34
Aspect Ratio	0.6	0.69	0.64	0.58

Table 3
Comparison between studied impact layers

Layer	Types of Ejecta	~ Size	Composition	Observed Textures	Vesicularity
K-T*	splash form	distal: 0.25mm proximal 0.9mm-1.1mm	K-spar, CPX, spinels	olivine ghosts, radial, flow bands at proximal sites	at proximal sites
Carawine**	splash form angular	angular:≤11 mm splash forms: 0.25mm-2.5mm	K-spar, quartz (chert), muscovite, carbonate, opaques	radial, internally random, flow bands, clear spots and central spot	95% of angular pop.
Jeerinah#	splash forms angular	splash form: up to 0.83mm angular:	K-spar, quartz (chert), sheet silicates, carbonate	radial, internally random, clear spots and a central spot	n/a
Wittenoom$	splash forms angular	1.7mm	K-spar, oxides, carbonate	radial, flow bands in angular, clear spots and central spot	n/a
S4	splash forms angular	splash form: 1.4mm (major axis) angular: 1.1mm (major axis)	K-spar, stilpnomelane (oxidized and unoxidized), calcite, opaques	radial, internally random, eccentric patterns (flow banded), central spot	vesicles in splash forms and angular grains

*(Smit et al., 1992; Smit, 1999)
**(Simonson et al., 2000b)
#(Simonson et al., 2000a)
&(Simonson, 1992)

References

Bakatt, Aa, Saad, E.E., Adiga, R., Sousanpour, W., Barkatt, Al. and Alterescu, S. 1986. Leaching of microtektite glass compositions in seawater. *Advances in Ceramics* **20**, p. 681-687.

Bryan, W. 1972. Morphology of quench crystals in submarine basalts. *Journal of Geophysical Research* **77**, p. 5812-5819.

Byerly, G.R. and Lowe, D.R. 1994. Spinel from Archean impact spherules. *Geochimica et Cosmochimica Acta* **50**, p. 3469-3486.

Chadwick, B., Claeys, P. and Simonson, B. 2001. New evidence for a large Paleoproterozoic impact: spherules in a dolomite layer in the Ketilidian orogen, South Greenland. *Journal of Geological Society, London* **158**, p. 331-340.

Chapman, C.R. and Morrison, D. 1994. Impacts on the Earth by asteroids and comets: assessing the hazards. *Nature* **367**, p. 33-40.

Gelinas, L. and Brooks C. 1974. Archean quench-texture tholeiites. *Canadian Journal of Earth Sciences* **11**, p. 324-340.

Gibb, F.G. 1974. Supercooling and the crystallization of plagioclase from a basaltic magma. *Mineralogic Magazine* **39**, p. 641-653.

Glass, B.P. 1984. Solution of naturally-occurring glasses in the geological environment. *Journal of Non-Crystalline Solids* **97**, p. 265-286.

Glass, B.P. 1986. Solution of natural glasses in the geological environment. *Advances in Ceramics* **20**, p. 723-732.

Glass, B.P., Muenow, D.W., Bohor, B.F. and Meeker, G.P. 1997. Fragmentation and hydration of tektites and microtektites. *Meteoritics and Planetary Science* **32**, p. 333-341.

Hassler, S.W. 1993. Depositional history of the Main Tuff Interval of the Wittenoom Formation, late Archean-early Proterozoic Hamersley Group, Western Australia. *Precambrian Research* **60**, p. 337-359.

Hassler S.W. and Simonson B.M. 2001. The sedimentary record of extraterrestrial impacts in deep-shelf environments: evidence from the early Precambrian. *Journal of Geology* **109**, p. 1-19.

LaBerge, G.L. 1966. Altered pyroclastic rocks in iron-formation if the Hamersley Range, Western Australia. *Economic Geology* **61**, p. 147-161.

Lofgren, G. 1971. Devitrified glass fragments from Apollo 11 and Apollo 12 lunar samples. *Proceedings from the Second Lunar Science Conference* **1**, p. 949-955.

Lofgren, G. 1971. Experimentally produced devitrification textures in natural rhyolitic glass. *Geological Society of America Bulletin* **82**, p. 111-124.

Lofgren, G. 1971. Spherulitic textures in glassy and crystalline rocks. *Journal of Geophysical Research* **76**, p. 5635-5648.

Lofgren, G. 1977. Dynamic crystallization experiments bearing on the origin of textures in impact-generated liquids. *Proceedings of the Lunar Science Conference* **8**, p. 2079-2095.

Lofgren, G. 1980. Experimental studies on the dynamic crystallization of silicate melts. *In*: Hargraves, R.B. ed. *Physics of Magmatic Processes*. pp 487-551. Princeton University Press, Princeton.

Lofgren, G. 1983. Effect of heterogeneous nucleation on basaltic textures: a dynamic crystallization study. *Journal of Petrology* **24**, p. 229-255.

Lofgren, G. and Donaldson, C.H. 1975. Curved branching crystals and differentiation in comb-layered rocks. *Contributions to Mineralogy and Petrology* **49**, p. 309-319.

MacDonald, I. and Simonson, B.M. 2002. PGE anomalies detected in tow more 2.5-2.6 billion year-old spherule layers in the Hamersley Basin of Western Australia. *Lunar and Planetary Science Conference* **33**, abstratct #1250.

Margolis, S., Claeys, P. and Kyte, F.T. 1991. Microtektites, microkrystites, and spinels from a late Pliocene asteroid impact in the southern ocean. *Science* **251**, p. 1594-1597.

Martinez Ruiz, F., Ortega Huertas, M., Palomo, I. and Acquafredda, P. 1997. Quench textures in altered spherules from the Cretaceous-Tertiary boundary layer at Agost and Caravaca, SE Spain. *Sedimentary Geology* **113**, p. 137-147.

Melosh, H.J. and Vickery, A.M. 1991. Melt droplet formation in energetic impact events. *Nature* **350**, p. 494-496.

Pearce, T.H. 1974. Quench plagioclase from some Archean basalts. *Canadian Journal of Earth Sciences* **11**, p. 715-719.

Pearce, T.H. and Donaldson, J.A. 1974. Proterozoic quench-texture basalts from the Labrador geosyncline. *Canadian Journal of Earth Sciences* **11**, p. 1611-1615.

Pettijohn, F.J. 1949. Sedimentary Rocks (1st ed.). Harper & Brothers, New York.

Pope, K.O. 2002. Impact dust not the cause of the Cretaceous-Tertiary mass extinction. *Geology* **30**, p. 99-102.

Ruzicka, A., Snyder, G.A. and Taylor, L.A. 2000. Crystal-bearing lunar spherules: impact melting of the Moon's crust and implications for the origin of meteoritic chondrules. *Meteoritics and Planetary Science* **35**, p. 173-192.

Simonson, B.M. 1992. Geological evidence for a strewn field of impact spherules in the early Precambrian Hamersley Basin of Western Australia. *Geological Society of America Bulletin* **104**, p. 829-839.

Simonson, B.M. and Harnik, P. 2000. Have distal impact ejecta changed through geologic time? *Geology* **28**, p. 975-978.

Simonson, B.M., Davies, D. and Hassler, S.W. 2000. Discovery of a layer of probable impact melt spherules in the late Archean Jeerinah Formation, Fortescue Group, Western Australia. *Australian Journal of Earth Science* **47**, p. 315-325.

Simonson, B.M., Hassler, S.W. and Beukes, N.J. 1999. Late Archean impact spherule layer in South Africa that may correlate with a Western Australian layer. *In*: Dressler, B.O. and Sharpton V.L. eds. *Large Meteorite Impacts and Planetary Evolution: Boulder, Colorado, Geological Society of America Special Paper 339.*

Simonson, B.M., Hassler, S.W. and Schubel, K.A. 1993. Lithology and proposed revisions in stratigraphic nomenclature of the Wittenoom Formation (Dolomite) and overlying formations, Hamersley Group, Western Australia. *Geological Survey of Western Australia*, Report **34**, Professional Papers, p. 65-79.

Simonson, B.M., Hornstein, M. and Hassler, S. 2000. Particles in late Archean Carawine Dolomite (Western Australia) resemble Muong Nong-type tektites. *In*: Gilmour, I. and Koeberl, C. eds. *Impacts and the Early Earth Lecture Notes in Earth Sciences* **92**.

Simonson, B.M., Schubel, K.A. and Hassler, S.W. 1993. Carbonate sedimentology of the early Precambrian Hamersley Group of Western Australia. *Precambrian Research* **60**, p. 287-335.

Smit, J. 1999. Global stratigraphy of the Cretaceous-Tertiary boundary impact ejecta. *Annual Review of Earth and Planetary Science* **27**, p. 75-113.

Smit, J., Alvarez, W., Montanari, A., Swinburn, N., Van Kempen T.M., Klaver, G.T. and Lustenhouwer, W.J. 1992. Tektites and microkrystites at the Cretaceous-Tertiary boundary: Two strewn fields, one crater? *Proceedings of Lunar and Planetary Science* **22**, p. 88-100.

Symes, S.J.K, Sears, D.W.G, Akridge, D.G, Huang, S. and Benoit, P.H. 1998. The crystalline lunar spherules: their formation and implications for the origin of meteoritic chondrules. *Meteoritics and Planetary Science* **33**, p. 13-29.

Trendall, A.F. 1983. The Hamersley Basin. *In*: Trendall, A.F. and Morris, R.C. eds. *Iron Formation: Facts and Problems*. Amsterdam, Elseiver, p. 69-129.